Engineered mesenchymal stromal cell therapy during human lung *ex vivo* lung perfusion is compromised by acidic lung microenvironment

Antti I. Nykänen,[1] Andrea Mariscal,[1] Allen Duong,[1] Catalina Estrada,[2] Aadil Ali,[1] Olivia Hough,[1] Andrew Sage,[1] Bonnie T. Chao,[1] Manyin Chen,[1] Hemant Gokhale,[1] Hongchao Shan,[1] Xiaohui Bai,[1] Guan Zehong,[1] Jonathan Yeung,[1] Tom Waddell,[1] Tereza Martinu,[1] Stephen Juvet,[1] Marcelo Cypel,[1] Mingyao Liu,[1] John E. Davies,[3] and Shaf Keshavjee[1,3]

[1]Latner Thoracic Surgery Research Laboratories, Toronto General Hospital Research Institute, University Health Network and University of Toronto, 101 College Street, Toronto, ON M5G 1L7, Canada; [2]Tissue Regeneration Therapeutics, 790 Bay Street, Toronto, ON M5G 1N8, Canada; [3]Institute of Biomedical Engineering, University of Toronto, 164 College St, Toronto, ON M5S 3G9, Canada

***Ex vivo* lung perfusion (EVLP) is an excellent platform to apply novel therapeutics, such as gene and cell therapies, before lung transplantation. We investigated the concept of human donor lung engineering during EVLP by combining gene and cell therapies. Premodified cryopreserved mesenchymal stromal cells with augmented anti-inflammatory interleukin-10 production (MSC^IL-10) were administered during EVLP to human lungs that had various degrees of underlying lung injury. Cryopreserved MSC^IL-10 had excellent viability, and they immediately and efficiently elevated perfusate and lung tissue IL-10 levels during EVLP. However, MSC^IL-10 function was compromised by the poor metabolic conditions present in the most damaged lungs. Similarly, exposing cultured MSC^IL-10 to poor metabolic, and especially acidic, conditions decreased their IL-10 production. In conclusion, we found that "off-the-shelf" MSC^IL-10 therapy of human lungs during EVLP is safe and feasible, and results in rapid IL-10 elevation, and that the acidic target-tissue microenvironment may compromise the efficacy of cell-based therapies.**

INTRODUCTION

Lung transplantation is a life-saving operation for many patients with end-stage lung disease, and the number of lung transplantations is constantly increasing with about 4,500 lung transplants reported to the International Society of Heart and Lung Transplantation each year.[1] Although lung transplant results have been improving over time, there is still lack of suitable donor organs, and short- and long-term results are limited by primary graft dysfunction, immunological complications, side effects of immunosuppressive drugs, and the development of chronic lung allograft dysfunction.[1–4] Novel therapeutic strategies that improve donor lung quality, or that protect and immunologically modulate the donor organ, are needed to further improve lung transplant results.

Normothermic acellular *ex vivo* lung perfusion (EVLP) is an innovative approach to assess donor lung quality outside the body before

transplantation, and it is used to safely increase the number of transplants.[5–7] EVLP can also be used as a platform to apply novel therapeutics during the *ex vivo* time.[5] Although lungs with specific injury, such as pulmonary embolism, have been successfully repaired during EVLP,[8] more universal lung repair strategies would significantly increase the organ pool for transplantation. In addition, successful protective and immunological engineering could be applied to standard, non-damaged, donor lungs to improve short- and long-term transplant results.

Gene and cell therapies have both been successfully implemented during EVLP in pre-clinical models,[9] but both strategies have their shortcomings. Gene therapy during EVLP generally aims to genetically modify donor cells to produce therapeutic factors, such as anti-inflammatory proteins, before the lung is transplanted.[10] However, viral gene vectors such as recombinant adenoviruses can induce inflammation,[11,12] which would be problematic in clinical transplantation. In addition, although adenoviral transfection is rapid, it takes up to 8–9 h to achieve measurable therapeutic interleukin-10 (IL-10) protein levels after airway delivery of adenoviral vectors encoding anti-inflammatory IL-10 (AdIL-10) in large-animal[13] and human-rejected lung EVLP experiments,[14] far longer than the 4- to 6-h duration of current standard clinical EVLP.[5]

Mesenchymal stromal cells (MSCs) reside in many tissues and participate in repair and immunomodulation primarily through paracrine mechanisms.[15,16] Anti-inflammatory properties of MSCs have made them attractive for various cell-based therapies,[15,17] and phase 1 studies in lung transplant patients with established chronic lung allograft
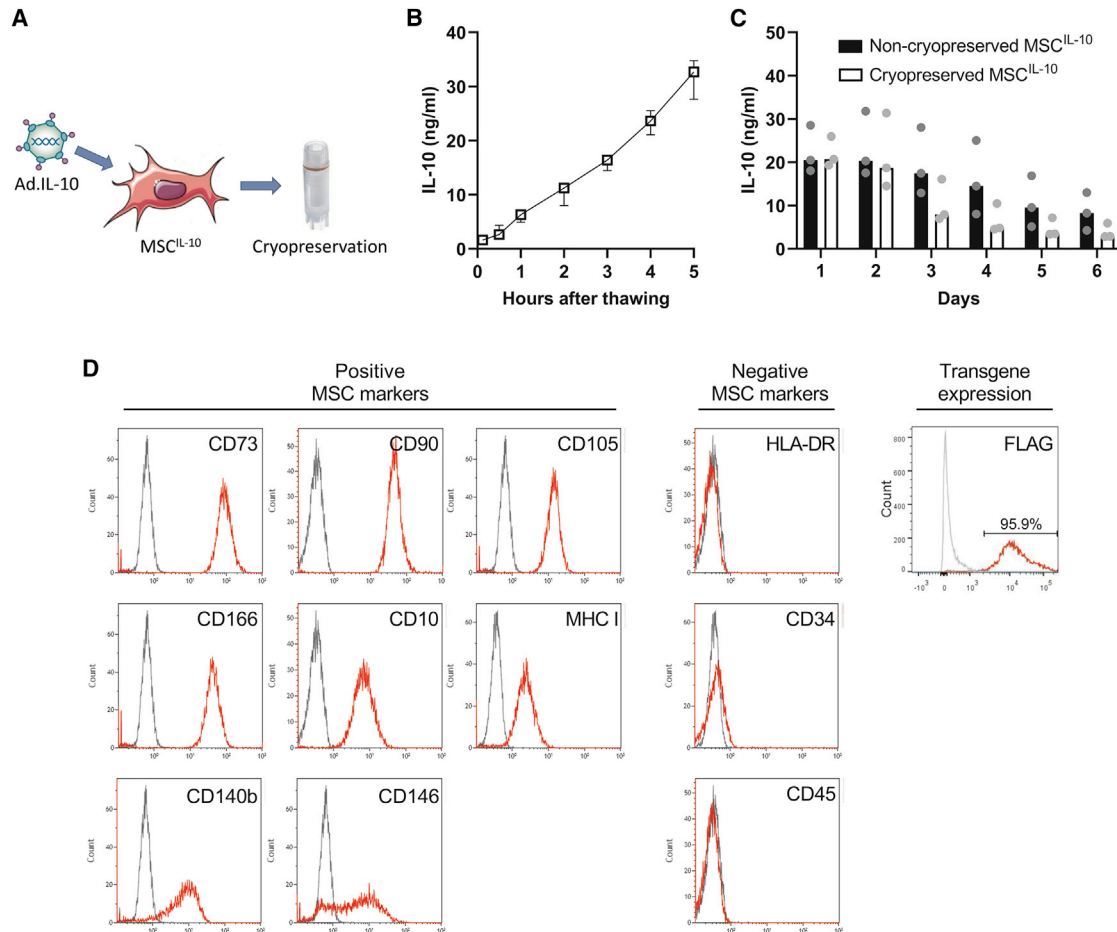
Figure 1. Cryopreserved MSC[IL-10] rapidly produce IL-10 *in vitro*

(A) Mesenchymal stromal cells (MSCs) isolated and expanded from human umbilical cord perivascular cells were transduced with recombinant adenovirus vectors encoding interleukin-10 (IL-10), and the engineered MSC[IL-10] were cryopreserved 2 days after transfection at the peak of their IL-10 transgene expression. To determine the IL-10 production of the engineered cells, MSC[IL-10] were cultured, and the secreted IL-10 was determined by ELISA. (B) Cryopreserved MSC[IL-10] started to produce IL-10 in minutes after thawing and the IL-10 secretion remained constant for 5 h (n = 3). (C) Daily IL-10 production of cryopreserved and non-cryopreserved MSC[IL-10] was similar and stable for 2 days and gradually declined thereafter (n = 3). (D) FACS analysis revealed that the engineered and cryopreserved MSC[IL-10] retained the typical MSC cell surface marker pattern, and almost all cryopreserved MSC[IL-10] were positive for FLAG tag, indicating high adenoviral vector transduction efficiency. Data median ± range (B), or median and individual values and analyzed by a Mann-Whitney test (C). Ad, adenovirus.

dysfunction have been conducted.[18,19] MSCs have also been used in various lung injury models[20–23] and in small clinical trials for acute respiratory distress syndrome (ARDS),[24–27] including patients with coronavirus disease 2019 (COVID-19).[28,29] We have previously used unmodified MSCs in EVLP and lung transplant experiments and found that intravascular administration was better than airway delivery.[30] MSC therapy decreased perfusate IL-8 levels during pig EVLP,[30] and it inhibited ischemia-reperfusion injury after pig lung transplantation.[31]

Here, we combined cell and gene therapies and investigated the concept of donor lung engineering during EVLP with genetically modified MSCs using highly translational models. Our overall goal is to determine whether genetically modified MSCs could be used to repair damaged lungs and therefore to increase the donor pool,

and to immunomodulate donor lungs and to consequently improve lung transplant results. Specific objectives for the current study were to investigate the safety and feasibility of genetically engineered MSC administration to human lungs during EVLP. Human umbilical cord perivascular MSCs were premodified to produce IL-10. These cryopreserved MSC[IL-10] were then administered during EVLP to human lungs rejected from clinical transplantation. This "off-the-shelf" therapy was feasible and safe, and it resulted in a rapid IL-10 increase in a time frame that is well suited for clinical ELVP. Interestingly, poor metabolic, and especially acidic, conditions in the severely damaged human lungs compromised MSC[IL-10] function, indicating that the local target-tissue metabolic microenvironment affects cell-based therapies in lung transplantation, and possibly also in other indications such as ARDS.

Table 1. Donor demographics and treatment allocation

	Case #1	Case #2	Case #3	Case #4	Case #5
Age, years	46	54	31	49	23
Sex	Male	female	female	male	female
TLC, L	7.49	6.08	5.25	8.39	5.09
Donor type	DCD	DBD	DCD	DBD	DBD
Cause of death	choking	overdose	overdose	choking	drowning
Smoking, pack-years	30	13	20	3	0
Main lung injury	LLL aspiration pneumonia and consolidation	RLL aspiration pneumonia	bilateral aspiration pneumonia	RLL aspiration pneumonia	LL necrotic areas
Last P/F ratio, mmHg	458	260	181	97	472
Bronchoscopy	left aspiration	bilateral aspiration	bilateral aspiration	RLL thick secretions	mild secretions
Microbiological finding					
Right lung perfusate	*Stenotrophomonas maltophilia* (R)	no growth	*Enterobacter cloacae* (R)	no growth	no growth
Left lung perfusate	*Enterococcus faecium* (R) and *Enterobacter cloacae* complex (R)	*Candida glabrata*	*Bordetella hinzii*	no growth	no growth
Treatment allocation					
Right lung	control	40×10^6 MSC^{IL-10}	control	not used	control
Left lung	40×10^6 MSC^{IL-10}	control	40×10^6 MSC^{IL-10}	40×10^6 MSC^{IL-10}	40×10^6 MSC^{IL-10}

DBD, donation after brain death; DCD, donation after circulatory death; IL-10, interleukin-10; LLL, left lower lobe; MSC, mesenchymal stromal cell; P/F ratio, ratio of arterial oxygen partial pressure to fractional inspired oxygen; R, multiresistant strain; RLL, right lower lobe.

RESULTS

Engineered and cryopreserved MSC^{IL-10} produce IL-10 rapidly after thawing *in vitro*

To generate genetically modified MSC^{IL-10} that could be used in an off-the-shelf manner during EVLP, human umbilical cord perivascular cells were isolated and expanded, transduced with second-generation AdIL-10 for 24 h, and cryopreserved 48 h after transduction (Figure 1A). The function of the cryopreserved MSC^{IL-10} was evaluated *in vitro* by plating them and measuring the secreted IL-10 protein. Significant IL-10 elevation was detected within 5 min of MSC^{IL-10} thawing, and IL-10 levels increased constantly for at least 5 h (Figure 1B). To evaluate the effect of cryopreservation on IL-10 transgene expression, cryopreserved and non-cryopreserved MSC^{IL-10} were compared for 6 days. Daily IL-10 production of both cell types was similar and stable for 2 days, and gradually declined thereafter with increased levels still detected at 6 days (Figure 1C). Cell viability after thawing was more than 90% (Table S1), and fluorescence-activated cell sorting (FACS) analysis revealed that the cryopreserved MSC^{IL-10} had retained their typical positive and negative MSC surface marker profiles (Figure 1D).[32] In addition, almost all cryopreserved MSC^{IL-10} were immunoreactive for FLAG tag, attached to the IL-10 transgene, indicating high transduction efficiency (Figure 1D).

EVLP perfusate IL-10 levels are rapidly and markedly elevated after administration of cryopreserved MSC^{IL-10} to human lungs during EVLP

Human double lungs rejected from clinical transplantation (Table 1; Figure S1) were split, and each lung was connected to a separate EVLP circuit for 12 h (Figures 2A and 2B). At the time of EVLP initiation, 40×10^6 MSC^{IL-10} were thawed and reconstituted to 20 mL of EVLP perfusate and administered randomly to one lung through the pulmonary artery 1 h after EVLP start (Table S1). The contralateral lung received 20 mL of EVLP perfusate and served as the control. To determine MSC^{IL-10} transgene production during EVLP, we measured IL-10 protein levels with ELISA from perfusate samples collected during the course of the 12-h EVLP. Control group EVLP perfusate IL-10 levels (Figure 2C) were low at 1 h (median 2 interquartile range [IRQ] 16 pg/mL), peaked to slightly higher levels at 6 h (median 115 IRQ 139 pg/mL), and remained slightly elevated at 12 h (median 66 IRQ 65 pg/mL). MSC^{IL-10} group EVLP perfusate IL-10 levels were low at 1 h (median 0 IRQ 50 pg/mL), markedly elevated 5 min after MSC^{IL-10} administration (median 1,147 IRQ 753 pg/mL), continued to increase, peaking at 6 h (median 5,190 IRQ 9,193 pg/mL), and remained increased at 12 h (median 4,164 IRQ 7,480 pg/mL) with the median IL-10 levels being almost 100-fold compared to the control group.

MSC^{IL-10} delivered during EVLP are retained in the lung and elevate lung tissue IL-10 levels

As MSC^{IL-10} treatment efficiently elevated perfusate IL-10 levels, we next determined whether a similar IL-10 increase occurs at the tissue level by evaluating lung tissue samples. Lung IL-10 levels were low in both groups before EVLP start and remained low in the control group during EVLP (Figure 2D). In contrast, MSC^{IL-10} treatment increased IL-10 in lung tissue to about 20 pg/mg lung protein (Figure 2D), with similar levels found in different anatomical lung
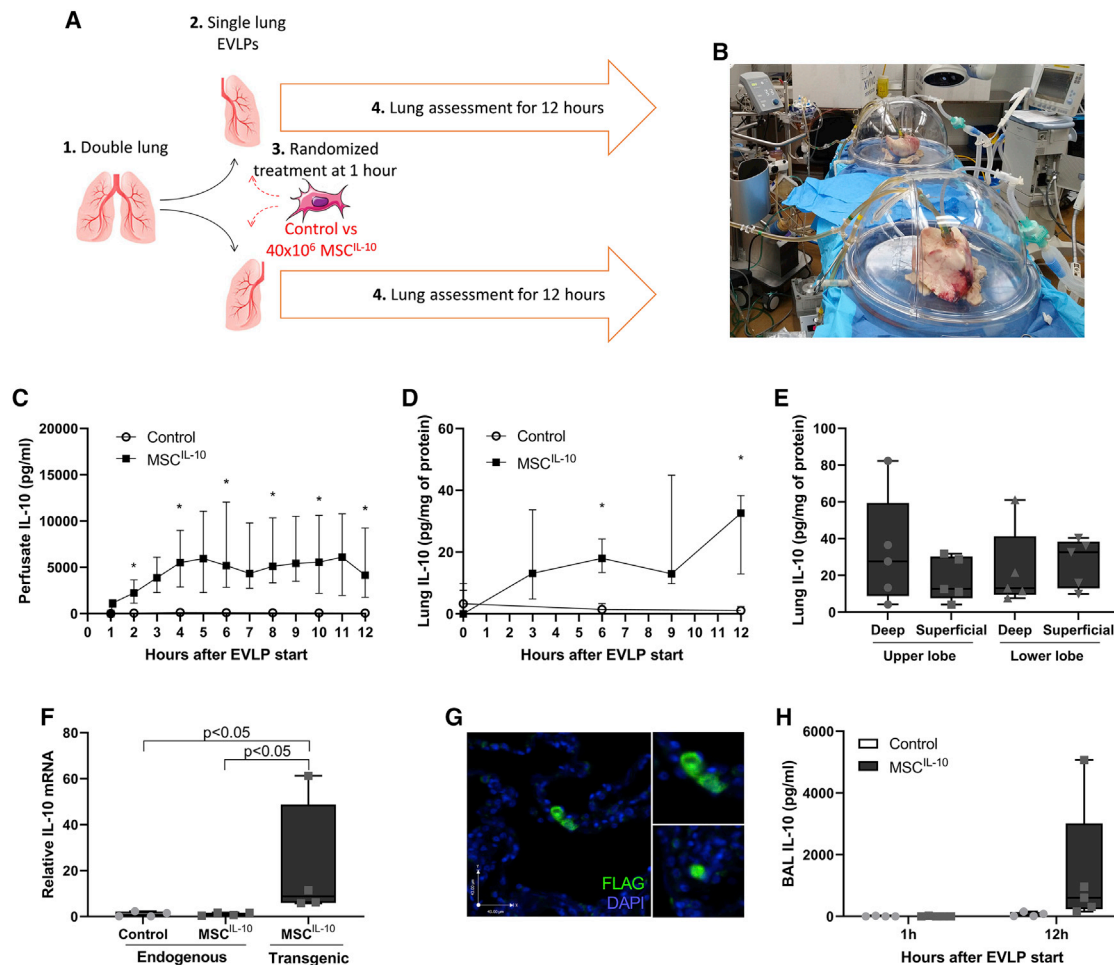
Figure 2. MSC^IL-10 treatment during human EVLP results in rapid and sustained IL-10 elevation

(A and B) Human double lungs rejected from clinical transplantation were split (n = 5), and the right and left lungs were connected to separate single-lung *ex vivo* lung perfusion (EVLP) circuits for 12 h. For each case, one lung was randomized to receive 40×10^6 MSC^IL-10 through the pulmonary artery (n = 5) 1 h after EVLP start, while the contralateral lung served as the control (n = 4). In one of these cases, only one lung was connected to EVLP and received MSC^IL-10, while the contralateral lung was excluded due to lung quality issues and a clinical concern that it was too damaged to last the planned 12-h EVLP experiment. (C) ELVP perfusate protein IL-10 levels were rapidly elevated already 5 min after MSC^IL-10 delivery, increased gradually, and plateaued at 6 h in the treatment group but remained low in the control group. (D) Lung tissue IL-10 protein levels remained elevated for 12 h in the treatment group, and (E) no significant IL-10 level differences were detected in discrete lung areas. (F) Lung tissue mRNA levels were analyzed using RT-PCR with primers specific for endogenous or transgenic IL-10 mRNA. Gene expression was determined relative to the Ppia housekeeping gene and normalized against endogenous IL-10 mRNA levels. (G) Immunostaining showed MSC^IL-10 expressing the IL-10 transgene (FLAG tag) retained in the MSC^IL-10-treated lungs. The upper inset shows a higher magnification view of the two adjacent MSC^IL-10 cells, and the lower inset shows an example of a single MSC^IL-10. (H) Bronchoalveolar lavage (BAL) IL-10 protein levels before MSC^IL-10 cell administration and at the end of EVLP. Data are expressed as median ± interquartile range (C and D) or as a boxplot with the box extending from the 25th to 75th percentile and showing the medium, whiskers extending to minimum and maximum values, and individual values plotted (E, F, and H), and analyzed by a Mann-Whitney test (C, D, and H) or Kruskal-Wallis test (E and F), and two-stage step-up method of Benjamini, Krieger, and Yekutieli for multiple comparisons. *$p < 0.05$.

locations (Figure 2E). To confirm IL-10 production at the mRNA level, and to determine the source of the elevated IL-10 in the lungs, we further analyzed lung samples using RT-PCR with primer sets specific for endogenous or transgenic IL-10 mRNA. Endogenous IL-10 mRNA levels were low in both groups (Figure 2F). Transgenic IL-10 mRNA was not detectable in the control group, but the levels were profoundly elevated in lungs treated with MSC^IL-10 cells and were 15-fold higher than endogenous IL-10 mRNA (Figure 2F). Im-

munostaining for the FLAG tag was performed to identify MSC^IL-10 and their transgene expression in lung tissue. No FLAG+ cells were detected in samples taken before MSC^IL-10 administration, or from the control group. In contrast, FLAG+ cells were present after MSC^IL-10 administration (Figure 2G), indicating efficient lung retention similar to our previous findings with unmodified MSCs.[30,31] IL-10 levels in bronchoalveolar lavage fluid were also elevated at the end of the EVLP procedure (Figure 2H), possibly
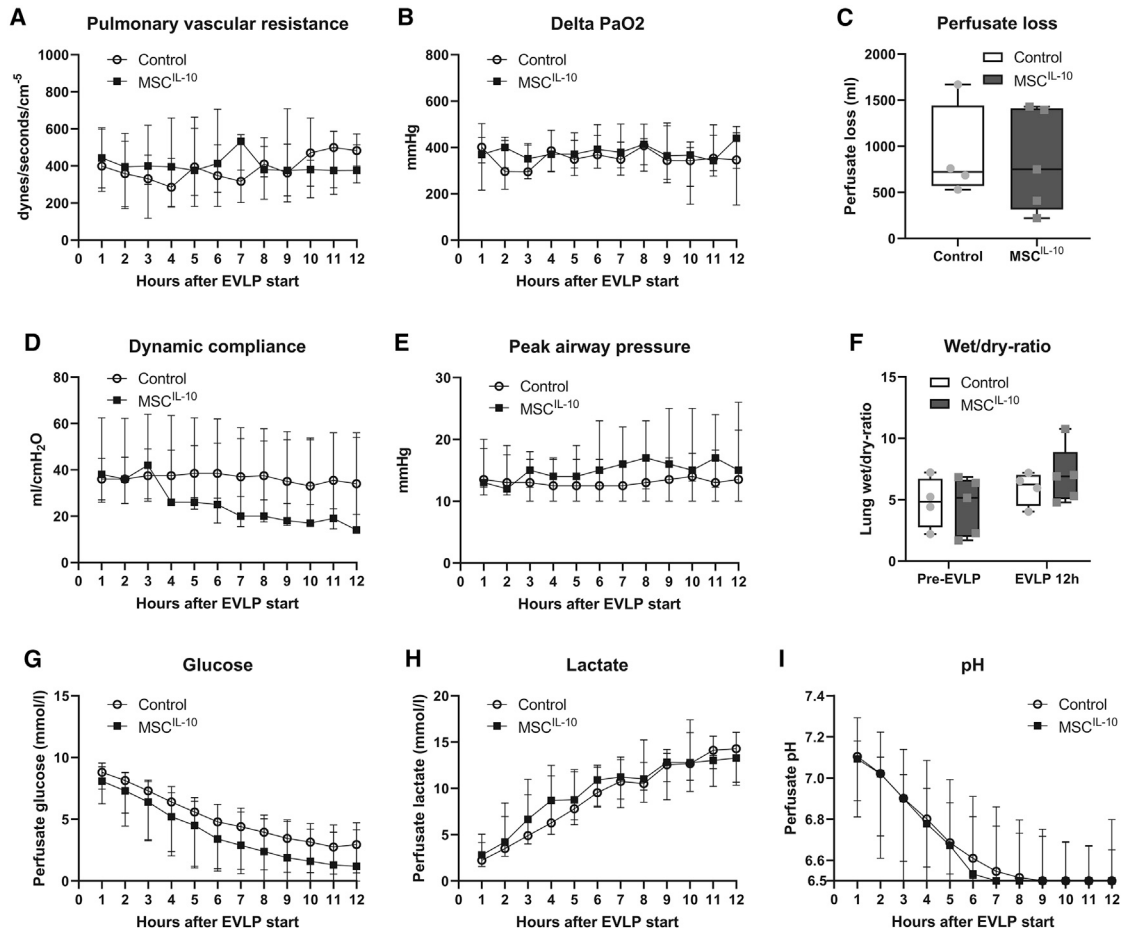
Figure 3. Lung function and metabolic parameters during EVLP

(A–I) Lung function was assessed and perfusate samples were obtained every hour during the 12-h EVLP. No significant differences were detected between the control group (n = 4) and the MSC[IL-10] group (n = 5) in (A) pulmonary vascular resistance, (B) ΔPaO_2 (left atrium perfusate PaO2 – pulmonary artery perfusate PaO2), (C) total perfusate loss during EVLP, (D) dynamic compliance, (E) peak airway pressure, (F) lung wet/dry ratio, (G) perfusate glucose, (H) perfusate lactate, or (I) perfusate pH. Data expressed as median ± interquartile range (A, B, D, E, and G–I) or as boxplot with the box extending from 25th to 75th percentile and showing the medium, whiskers extending to minimum and maximum values, and individual values plotted (C and F), and analyzed by two-way ANOVA (A, B, and D–I) or by a Mann-Whitney test (C).

due to the transgenic protein crossing the epithelial barrier, or due to MSC[IL-10] migration to the alveolar space.

MSC[IL-10] administration during EVLP does not change lung function parameters

We next compared the functional parameters of control and MSC[IL-10] group lungs (median values are given in Figure 3, and individual values of each case are included in Figure S2). Importantly, administration of 40×10^6 MSC[IL-10] did not increase pulmonary vascular resistance (Figure 3A). Previously, MSC doses several fold higher than the current dose were associated with increased pulmonary vascular resistance.[30] In addition, no differences in lung oxygenation capacity, compliance, airway pressure, perfusate loss, or the tissue wet/dry ratio between the groups were detected (Figures 3B–3F), indicating safety of the 40×10^6 MSC[IL-10] administration. Also, no differences in levels of proinflammatory perfusate cytokines were detected (Figure S3).

Poor metabolic conditions during EVLP correlate with low achieved lung tissue IL-10 levels at the end of EVLP by MSC[IL-10] treatment

Throughout the 12-h EVLP, worsening of lung metabolic conditions was observed, indicated by an ongoing decrease in perfusate glucose (Figure 3G) and pH (Figure 3I), and by an increase in perfusate lactate (Figure 3H). Although the median values between groups were similar, there was significant variance between cases, and even between the left and right lung of each case, consistent with the heterogeneous quality of the lungs that were originally rejected from clinical transplantation (Table 1; Figure S1). The most damaged lungs had a specific pattern of perfusate metabolic factors: glucose and pH were initially low, and declined quickly, whereas lactate was initially high, and increased rapidly (Figure S4, case 1 right lung, and case 3 right and left lungs). This finding was likely contributed to by infection, as perfusate samples of these severely
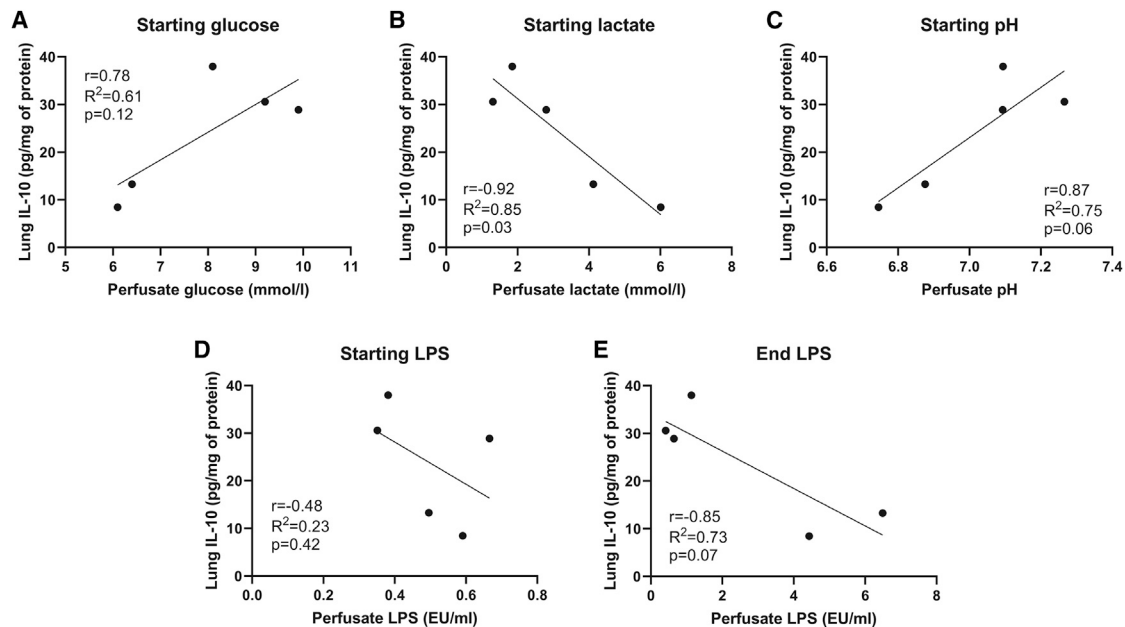
Figure 4. Poor metabolic conditions during EVLP correlate with low achieved lung tissue IL-10 levels

(A–E) In cases receiving MSC^IL-10 treatment (n = 5), EVLP perfusate metabolic factors were correlated with the achieved lung tissue IL-10 levels. Correlation of starting perfusate (EVLP 1 h) (A) glucose, (B) lactate, (C) pH, and (D) LPS, and correlation of end perfusate (EVLP 12 h) (E) LPS, with EVLP 12-h lung tissue IL-10 protein levels. Analyzed by linear regression and Pearson coefficient test. EU, endotoxin unit.

injured lungs had antibiotic-resistant bacteria growth in microbiological cultures (Table 1) and concomitant high lipopolysaccharide (LPS) levels (Figure S4).

In order to evaluate MSC^IL-10 performance in the hostile microenvironment of damaged lungs, we next correlated EVLP metabolic conditions with the achieved lung tissue IL-10 levels at the end of EVLP, a surrogate indicator of MSC^IL-10 function. A significant negative correlation was observed between starting lactate and the 12-h lung IL-10 levels (Figure 4B), whereas a trend was observed with low starting glucose (Figure 4A), low pH (Figure 4C), and high-end LPS (Figure 4E), resulting in low tissue IL-10 levels at the end of EVLP.

Acidic lung microenvironment negatively affects IL-10 levels

To further explore whether the lung microenvironment affects MSC^IL-10 function, lung interstitial pH was measured with a pH microelectrode from tissue samples collected at the end of EVLP from various anatomical sites of the MSC^IL-10-treated lungs, and the tissue pH was correlated with IL-10 levels of the same lung samples. A significant correlation between acidic pH and low tissue IL-10 levels was found (Figure 5A), and samples with pH ≥6.3 had almost 3-fold higher IL-10 levels than did samples with pH <6.3 (Figure 5B). To visualize acidic lung areas, a cell-permeable, pH-sensitive fluorogenic probe pHrodo was used. pHrodo becomes fluorescent in an acidic environment,[33,34] and after incubation of lung tissue frozen sections with pHrodo, a more intense red fluorescence pHrodo signal was detected in samples with low pH (Figure 5C) than in samples with

higher pH (Figure 5D), reinforcing the findings of the lung interstitial pH measurements.

Exposure of MSC^IL-10 to human EVLP perfusate samples with poor metabolic conditions *in vitro* impairs IL-10 production

To better understand the effect of metabolic conditions on cell function, MSC^IL-10 were cultured for 4 h with human EVLP perfusate samples that had varying glucose, lactate, and pH levels (Figure 6A). Although IL-10 secretion by MSC^IL-10 increased over time, it was severely blunted when MSC^IL-10 were cultured in the worst metabolic conditions (Figure 6A), especially in samples with low glucose or pH (Figure 6B). To further evaluate which metabolic parameters were important for MSC^IL-10 function, the achieved IL-10 levels were correlated with the glucose (Figure 6C), lactate (Figure 6D), and pH levels (Figure 6E) of the respective culture conditions. A clear correlation between IL-10 and each of these factors was seen, with higher glucose, lower lactate, and more physiological pH correlating with higher IL-10 production while hypoglycemia, lactatemia, and acidity resulted in lower IL-10 levels. To address whether the cytokine environment also contributes to MSC^IL-10 function, we measured pro-inflammatory and damage-related factors in the samples used for the experiment and correlated their levels with the achieved IL-10 (Figure S5). Increased IL-6 and IL-8, and especially elevated soluble tumor necrosis factor receptor 1 (sTNFR1) and soluble triggering receptor expressed by myeloid cells 1 (sTREM1), were associated with low IL-10 production (Figure S5), whereas no significant correlation was found between IL-1β, endothelin-1, or granulocyte-macrophage colony-stimulating factor (GM-CSF) and IL-10 levels (Figure S5).
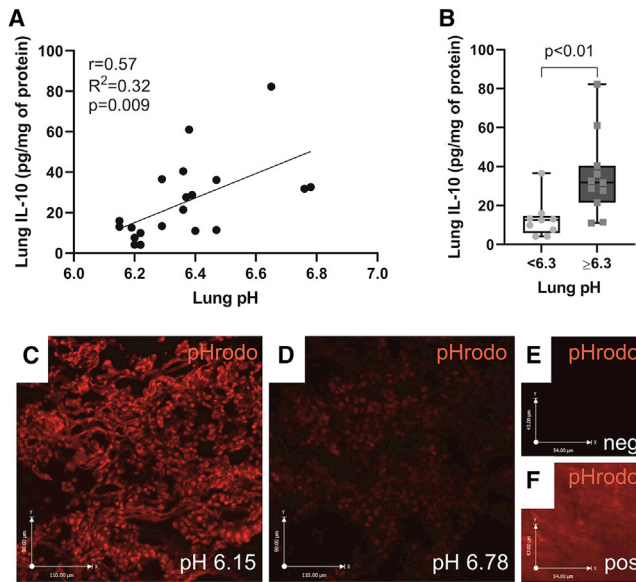
Figure 5. Lung tissue interstitial acidity correlates with low IL-10 levels

Lung tissue interstitial pH was measured with a pH microelectrode from tissue samples collected at the end of EVLP from four different anatomical locations of each of the MSC^{IL-10}-treated lung (n = 20 samples from five lungs). (A) Correlation of lung interstitial pH with tissue IL-10 levels. (B) Lung IL-10 levels stratified according to tissue pH (pH < 6.3, n = 9 samples; pH ≥ 6.3, n = 11 samples). To visualize and localize acidic lung areas, lung tissue frozen sections were incubated with a pHrodo probe that becomes fluorescent in an acidic environment. (C) Lung samples with the lowest pH had more red pHrodo fluorescence than did (D) samples with a higher pH. (E) Low background was seen in lung samples before pHrodo incubation, whereas (F) intense fluorescence was detected in acidic gastric samples incubated with pHrodo. Data are expressed as a boxplot with the box extending from the 25th to 75th percentile and showing the medium, whiskers extending to minimum and maximum values, and individual values plotted and analyzed by a Mann-Whitney test (B), or by linear regression and a Pearson coefficient test (A).

Acidity decreases MSC^{IL-10} viability and IL-10 production *in vitro*

As glucose and pH were the metabolic factors that best correlated with MSC^{IL-10} function, we next exposed MSC^{IL-10} either to varying glucose concentrations or to varying pH levels for 4 h, while maintaining other culture conditions constant. MSC^{IL-10} cultured in media with high (25 mmol/L), low (5.5 mmol/L), or no glucose had similar cell viability (Figure 7A) and IL-10 secretion (Figure 7B). In contrast, when MSC^{IL-10} were exposed to varying pH levels, cell viability was compromised in severely acidic culture conditions (Figure 7C). In addition, compared to physiological extracellular pH 7.4, acidic pH inhibited MSC^{IL-10} IL-10 production with the most severe acidic conditions resulting in the lowest IL-10 levels.

DISCUSSION

We generated engineered MSCs and deployed them as gene therapy vehicles for lung protection. A translational human lung EVLP model was used, and the MSC^{IL-10} treatment strategy was designed so that the threshold for future clinical applications would be low. MSC^{IL-10} therapy during EVLP was feasible and safe, and it resulted in rapid and efficient IL-10 elevation in human lungs. Interestingly, MSC^{IL-10} were

sensitive to surrounding metabolic conditions, especially to acidity, which will be an important consideration when designing future cell-based therapies.

Cell and gene therapies have been improved over time, and both treatments have been successfully used in selected clinical situations.[35,36] The concept of combining cell and gene therapies has potential therapeutic, safety, and practical advantages.[15,37] MSCs home to injured sites and participate in repair and immunomodulation, mainly by secreting molecules and releasing extracellular vesicles.[15,16] Genetic engineering modifies MSCs so that, in addition to their normal secretome, they express a therapeutic transgene product, which potentially results in synergetic effects.[15,23,37–39] In the present report, MSCs were engineered to produce IL-10, a soluble anti-inflammatory protein that has been beneficial in various lung transplant models,[12,14,40,41] but other candidate genes, or a combination of genes, could also be used to achieve transplant protection and immunomodulation.[10] Previously, genetically modified MSCs have been used in small-animal ARDS models to improve MSC homing, or to target inflammation, apoptosis, or compromised alveolar barrier function.[37,42–44] Our present results indicate that genetically modified MSCs can be used in the human lung. Intravascular MSC^{IL-10} delivery resulted in lung MSC^{IL-10} retention, and efficient IL-10 elevation in EVLP perfusate, lung tissue, and bronchoalveolar lavage fluid. The paracrine secretion of IL-10 into all lung compartments, including the alveolar space, may be important, as alveolar macrophages have a critical role in lung ischemia-reperfusion injury[45] and are important mediators of the anti-inflammatory effects of IL-10.[46]

Vector-related insertional mutagenesis[47] and inflammation[11] have been the biggest safety issues for gene therapy. The strategy of using MSCs pretransduced with recombinant adenoviral vectors may largely circumvent these safety concerns. The risk for insertional mutagenesis with adenoviral vectors is minimal, as the transgene stays non-integrated.[47] However, adenoviral capsid proteins and nucleic acids evoke innate and adaptive immune responses that result in the elimination of the virus, the virally infected target cell, and the transgene expression.[11] Compared to direct delivery of AdIL-10 vectors to lungs, delivery of pretransduced MSC^{IL-10} may result in less inflammation, as the host exposure to adenoviral capsid proteins should be lower, and any anti-viral immune reaction would target MSC^{IL-10} instead of the lung cells. Although MSCs have been described as immunoprivileged, they also can evoke immune responses,[26] which is also a possibility in our treatment strategy, as third-party allogeneic MSCs derived from human umbilical cord perivascular cells were used. Ultimately, transplant experiments will be needed to determine potential anti-MSC^{IL-10} and anti-viral responses of the host, and the kinetics of MSC^{IL-10} viability and IL-10 transgene expression after lung transplantation. MSC aggregation in the target organ capillary bed is also a possible safety concern related to cell-based therapies.[15,17] In our previous pig EVLP experiments, intravascular delivery of 300×10^6 MSCs, but not lower MSC doses, was associated with increased pulmonary artery resistance.[30] Here, intravascular administration of 40×10^6 MSC^{IL-10} to a single
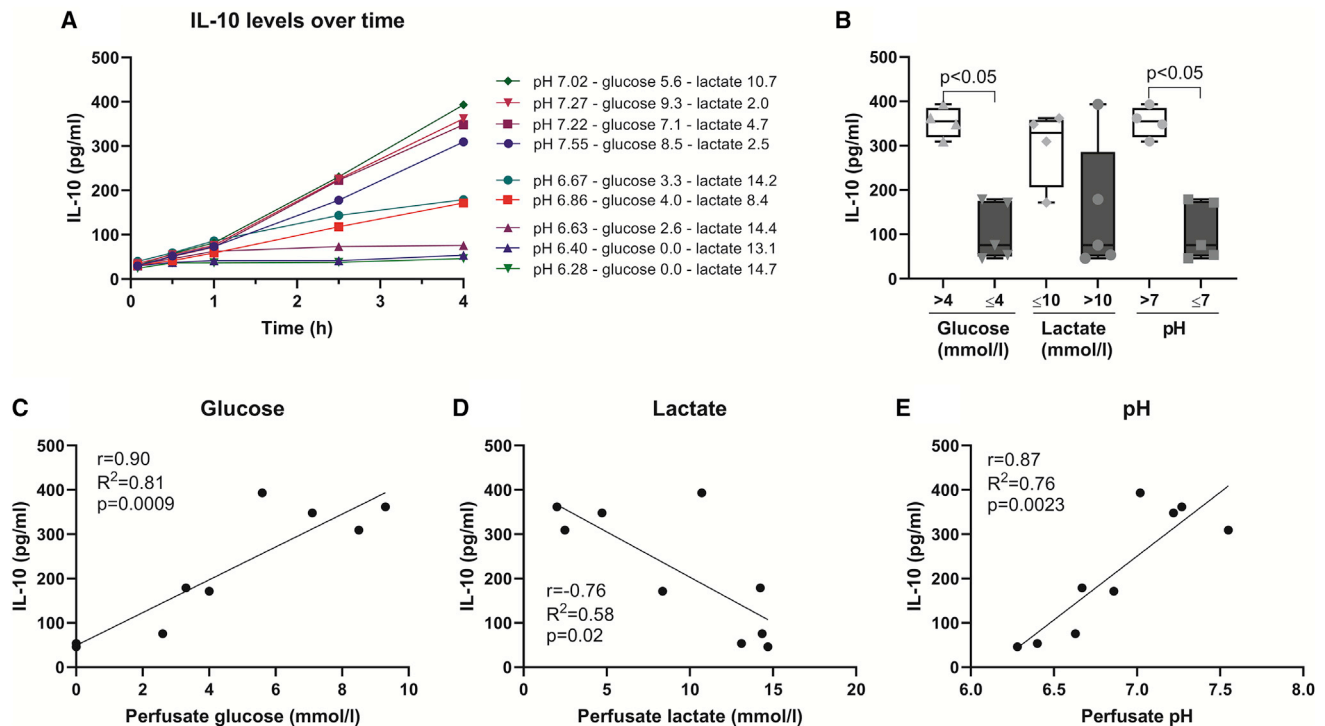
Figure 6. Poor perfusate metabolic conditions decrease MSC^{IL-10} IL-10 production *in vitro*

(A) MSC^{IL-10} were plated *in vitro*, cultured in nine different human EVLP perfusate samples, and IL-10 secretion was measured at 0.5, 1, 2.5, and 4 h. The nine samples used consisted of 1-, 6-, and 12-h perfusate samples of control group cases 1–3, resulting in a spectrum of different glucose, lactate, and pH conditions (individual metabolic values are given in the legend to A), and leading to increasing but varying IL-10 production by the MSC^{IL-10}. (B) Analysis of 4-h IL-10 levels stratified by low or high levels of glucose (cutoff of 4 mmol/L), lactate (cutoff of 10 mmol/L), or pH (cutoff of pH 7). (C–E) Correlation of 4-h IL-10 concentration with respective perfusate (C) glucose, (D) lactate, and (E) pH levels. Data are expressed as a boxplot with the box extending from the 25th to 75th percentile and showing the medium, whiskers extending to minimum and maximum values, and individual values plotted and analyzed by a Mann-Whitney test (B), or by linear regression and a Pearson coefficient test (C–E).

human lung did not increase pulmonary vascular resistance. This is consistent with clinical trials using intravenous MSC administration to lungs.[18,19,26]

The utilization of cryopreserved cells in an off-the-shelf manner significantly improves the clinical feasibility of engineered MSC therapy.[48] This approach is well suited for a clinical scenario, where the donor lung is connected to EVLP, considered for cell-based therapy for graft repair or modulation, and cryopreserved pre-engineered "ready-to-go" MSCs are administered during EVLP. However, although the practicability of this approach is evident, it is important that cryopreservation should not compromise efficacy. Importantly, we found that the cryopreserved MSC^{IL-10} had excellent viability,[26] expressed the usual MSC surface markers,[32] and secreted IL-10 within minutes after thawing *in vitro*, and after delivery to the lung, indicating that cryopreservation did not compromise MSC^{IL-10} function. Using pre-engineered MSCs as gene transfer vehicles has an additional translational advantage. When AdIL-10 vectors are delivered directly to the lung during EVLP, it takes up to 8–9 h to achieve therapeutic IL-10 levels,[13,14] and therefore the clinical EVLP duration would need to be extended. In contrast, MSC^{IL-10} therapy is compat-

ible with the shorter more standard clinical EVLP as a rapid IL-10 increase is achieved.

One unexpected, but important, finding of the current study was that MSC^{IL-10} were affected by poor metabolic conditions both *in vitro* and in the human lung. It is well documented that culture conditions have significant effects on MSC biology.[49] This can be utilized for therapeutic purposes, as MSCs can be primed, for example, with inflammatory factors or hypoxia, to augment their therapeutic effects in the target tissue.[49] The target tissue microenvironment can conversely affect MSC function,[50] and ultimately determine the outcome of MSC therapy. As an example, in a mouse ARDS model, MSC therapy after ventilator-induced lung injury resulted in beneficial effects, but cell delivery 2 days after acidic damage aggravated lung fibrosis.[23] In our study, severe acidity compromised the viability of cultured MSC^{IL-10}, and IL-10 secretion was blunted in pH 6.5, an acidity level that was present in the damaged human lungs of the study, and is also found during tissue injury,[51] ischemia,[52] infection,[53–55] ARSD,[56] or in tumors.[57] The finding that MSCs are sensitive to acidic conditions may thus have clinical significance for the efficacy of cell-based therapies targeting various organs, and several issues
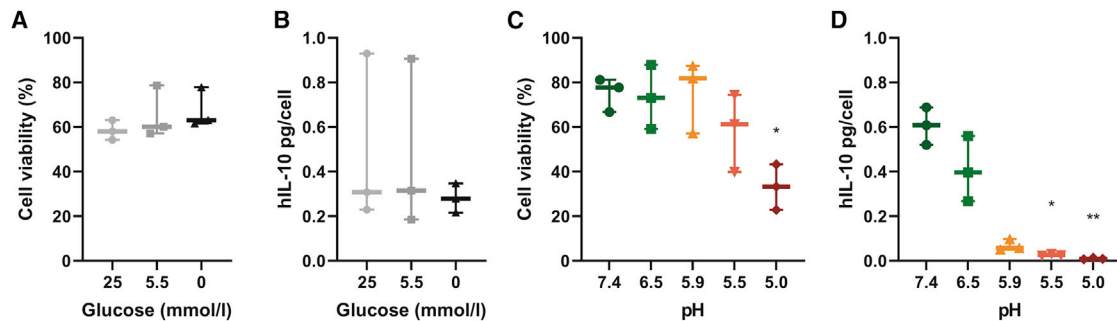
Figure 7. Acidity impairs MSC^{IL-10} IL-10 secretion *in vitro*

MSC^{IL-10} cells were subjected to varying glucose or varying pH conditions *in vitro* (n = 3 for each condition), and cell viability and IL-10 production were analyzed at 4 h. (A) MSC^{IL-10} cultured in DMEM media with high (25 mmol/L), low (5.5 mmol/L), or no glucose for 4 h had similar cell viability, and (B) no significant differences in IL-10 levels were detected. (C) When MSC^{IL-10} were cultured in perfusate with varying pH for 4 h, cell viability remained unchanged in slightly acidic conditions but was compromised in pH 5.0. (D) Compared to physiological extracellular pH 7.4, acidic pH inhibited MSC^{IL-10} IL-10 production with the most severe acidic conditions resulting in the lowest IL-10 levels. Graphs show the medium, whiskers extending to minimum and maximum values, and individual values, and data were analyzed by a Kruskal-Wallis test and two-stage step-up method of Benjamini, Krieger, and Yekutieli for multiple comparisons comparing respective conditions to glucose 25 mmol/L or pH 7.4 groups. *p < 0.05, **p < 0.01.

should be considered when designing MSC strategies for lungs. First, as a hostile lung microenvironment may compromise MSC function, therapeutic effects may be best achieved by excluding the most extreme lung injury. Second, strategies to optimize the target microenvironment could improve MSC effects. For example, acidity could be alleviated with sodium bicarbonate, ventilation strategies, or dialysis, or by treating any direct underlying cause such as infection. Third, similar to the findings related to priming with hypoxia,[49] MSCs could be potentially primed or engineered to better tolerate the unfavorable target-tissue microenvironment.

Although previous reports using IL-10 gene therapy or unmodified MSCs have during EVLP found beneficial effects in the lung, we did not observe significant differences in lung function or cytokine profile. We think this can at least in part be explained by the heterogeneous injury in the lungs used for the study. As we used lungs that were rejected from clinical transplantation, all lungs had quality concerns, and especially some lungs randomized to the MSC^{IL-10} group had severe lung injury. This helped us to investigate the effect of the level of lung injury on MSC^{IL-10} function, but most likely made it difficult to detect potential functional effects of the treatment. In future studies, we aim to use experimental large animal EVLP and transplant models with standardized, and less severe underlying lung injury, to delineate the potential protective and immunomodulatory effects of MSC^{IL-10}.

Differences in IL-10 gene therapy and MSC^{IL-10} therapy may also explain the lack of observed beneficial effects on lung function in the current study. Although MSC^{IL10} administration resulted in even higher lung tissue IL-10 levels than did adenoviral IL-10 delivery,[13,14] the underlying differences of these two IL-10 delivery methods may result in distinct biological outcomes. We found that MSC^{IL-10} were retained within the lung and likely affected neighboring cells through paracrine secretion of soluble IL-10. In contrast, airway delivery of adenoviral vectors encoding IL-10 primarily trans-

fects epithelial cells and alveolar macrophages, and reprograms them to produce IL-10.[13,14] The endogenous, gene therapy-mediated IL-10 production may thus generate more robust effects especially on epithelial cells and alveolar macrophages than the paracrine IL-10 secretion by MSC^{IL-10}. This difference may be important particularly due to the critical roles of alveolar macrophages and IL-10 in regulating lung ischemia-reperfusion injury.[45,58,59]

In conclusion, we generated and administered genetically modified MSCs to human lungs during EVLP to investigate the concept of donor lung engineering. This off-the-shelf therapy was feasible and safe, and resulted in rapid IL-10 increase in human lungs in a time frame that is well suitable for clinical translation. Interestingly, MSC^{IL-10} were sensitive to surrounding metabolic conditions, especially to acidity, which is an important consideration when designing future cell-based therapies.

MATERIALS AND METHODS
Experimental design
Human umbilical cord perivascular cells were genetically modified to produce IL-10 using AdIL-10 transduction (MSC^{IL-10}), and cryopreserved (Figure 1A). The function of cryopreserved MSC^{IL-10} was confirmed *in vitro*. Human double lungs rejected from clinical transplantation (n = 5) were split and connected to separate single-lung EVLP circuits for 12 h. One lung of each case was randomized to receive cryopreserved 40 × 10^6 MSC^{IL-10} through the pulmonary artery after the first hour on EVLP, while the contralateral lung served as the control (Figure 2A). Lung function parameters and perfusate samples were collected every hour, lung tissue samples every third hour, and bronchoalveolar lavage samples before MSC^{IL-10} administration and at 12 h. MSC^{IL-10} function during EVLP was determined by measuring EVLP perfusate, lung tissue, and bronchoalveolar lavage IL-10 protein levels. MSC^{IL-10} localization in lung tissue was determined by immunostaining for the FLAG tag attached to the IL-10 transgene. The effect of pH, glucose, lactate, and LPS on MSC^{IL-10}

function during EVLP was evaluated by correlating metabolic parameters with achieved lung tissue IL-10 levels. The effect of different metabolic conditions on MSC^{IL-10} function *in vitro* was studied by culturing MSC^{IL-10} with EVLP perfusate samples with various metabolic conditions, or by selectively modifying culture media glucose or pH. The study was approved by the University Health Network Research Ethics Board (06-0283) and Trillium Gift of Life Network.

MSC isolation and expansion

Human umbilical cords (UCs) from full-term, consenting donors undergoing caesarean section at Mount Sinai Hospital (Toronto, ON, Canada) were sourced with approval from ethics boards at both the University Toronto and Mount Sinai Hospital Research Centre for Women's and Infants' Health (RCWIH). The UC-derived MSCs were extracted using a proprietary methodology and provided by Tissue Regeneration Therapeutics (TRT) (Toronto, ON, Canada). Briefly, following removal of the amniotic epithelium using blunt dissection, the three cord vessels were separated along with their perivascular Wharton's jelly (WJ) tissue. The WJ tissue was stripped from the vessel walls, minced, and seeded in fibronectin-coated culture flasks, in Lonza TheraPEAK MSCGM-CD serum-free medium (Cedarlane, Burlington, ON, Canada) for 14 days to isolate cells. At harvest, the adherent cells were dissociated with TrypLE Express (Thermo Fisher Scientific, Waltham, MA, USA). Tissue fragments were strained, and cell suspension was collected and centrifuged for 10 min at $285 \times g$, after which the supernatant was discarded, the cells were washed, and the culture was expanded to P1 and cryopreserved as a master cell bank (MCB). Due to a disruption in the Lonza supply chain, the TheraPEAK MSCGM-CD medium was no longer available. As a result, MCB vials were later thawed into RoosterNourish MSC-XF medium (RoosterBio, Frederick, MD, USA) for expansion to P2 and stockpiled in liquid nitrogen.

Genetic engineering of MSCs

A premade human replication-incompetent (E1/E3 gene-deleted) recombinant adenovirus vector (type 5) with cytomegalovirus (CMV) promoter-driven expression of human IL-10 (including FLAG tag) was purchased from Vigene Biosciences (Rockville, MD, USA; no. VH869610). Cells were seeded at a density of 23×10^3 cells/cm^2 and 24 h later were exposed to the virus at a multiplicity of infection of 100 in 100 μL/cm^2 of RoosterNourish MSC-XF medium. After 24 h of incubation at 37°C, 5% CO_2, cells were washed with PBS three times and fresh growth medium was added. Engineered MSC^{IL-10} were harvested 48 h later and cryopreserved in liquid nitrogen for future use.

In vitro evaluation of engineered MSC^{IL-10}

IL-10 production of non-cryopreserved and cryopreserved MSC^{IL-10} was assessed by culturing 1×10^5 cells in 12-well plates in 1 mL of media at 37°C, 5% CO_2. After conditioning the medium for 24 h, it was collected daily for the determination and comparison of human IL-10 levels by ELISA (n = 3).

To study the secretory activity of cryopreserved cells after thaw, 54×10^3 MSC^{IL-10} were seeded in 12-mm Transwells with 3.0-μm pore membrane inserts (Corning Life Sciences, Corning, NY, USA) in a total of 2 mL of EVLP perfusate solution per well at 37°C, 5% CO_2. Samples were taken from the bottom compartment at 5 and 30 min and at 1–5 h. ELISA was performed to determine human IL-10 concentration (n = 3).

FACS analysis of both naive and MSC^{IL-10} was used to determine the expression of CD73, CD90, CD105, CD10, CD166 and CD140b, CD31, CD34, CD45, major histocompatibility complex class II (MHC class II) and to evaluate IL-10 transgene expression with anti-FLAG antibodies.

Human rejected lungs

Human donor lungs rejected from clinical transplantation were used in the study, from donors who consented for research. The lungs were procured by the Toronto Lung Transplant Program according to standard clinical protocols, including antegrade and retrograde lung flush with low potassium dextran solution (Perfadex, XVIVO Perfusion, Gothenburg, Sweden), and transported and stored at 4°C. Double lungs were split and connected to separate EVLP circuits. Each lung had varying levels of injury depending on the donor history (Table 1; Figure S1). In one case (case 4, Figure S1), the right lung with aspiration pneumonia and extensive atelectasis was not used for the experiment due to a clinical concern that it was too damaged to last the planned 12-h EVLP experiment, and only the left lung was connected to EVLP and received MSC^{IL-10}. The study therefore consists of four control lungs and five MSC^{IL-10} treatment lungs.

Single-lung EVLP

Each split lung was connected to a separate Toronto EVLP system, and EVLP and lung evaluation were performed according to standard clinical EVLP protocols.[60] Briefly, the atrial cannula was sutured to the donor atrium, pulmonary artery cannula was connected to the main pulmonary artery, a 7.5Fr endotracheal tube was inserted to the main bronchus on each side, and the lung was flushed retrogradely with low-potassium dextran solution (Perfadex). The EVLP circuit was primed with 1,500 mL of EVLP perfusate (LPD2A, United Therapeutics, Silver Spring, MD, USA in cases 1–4; Steen solution, XVIVO Perfusion, Gothenburg, Sweden in case 5; both perfusate solutions have identical composition), and heparin at 10,000 IU, methylprednisolone at 1 g, and antibiotics (cefazolin at 1 g in cases 1–3 and meropenem at 500 mg in cases 4 and 5). During the initial hour, EVLP flow was increased incrementally to 40% of the calculated total cardiac output, taking into consideration the adjustment for single-lung EVLP (left lung 40% and right lung 60% of the flow), temperature was gradually increased, and ventilation started at 32°C with tidal volume at 7 mL/kg, positive end-expiratory pressure (PEEP) at 5 cmH$_2$O, the fraction of inspired oxygen (FiO$_2$) of 0.21, and rate of 7 per min. Tidal volume was also adjusted for single-lung EVLP (40% for the left lung and 60% for the right lung). Lung function parameters and perfusate samples were taken every hour with challenge ventilatory settings of tidal volume at 10 mL/kg, PEEP at 5 cmH$_2$O, FiO$_2$ of 1.0, and rate of 10 per min. Perfusate pH, partial pressure of CO_2 (pCO$_2$), partial pressure of O_2 (pO$_2$), glucose, and lactate

were immediately analyzed with a point-of-care system (RAPIDPoint 500 blood gas system, Siemens Healthineers, Erlangen, Germany) and cOmplete, and supernatant and cell fractions of perfusate were stored at −80°C and −150°C (cell fractions). EVLP protocol consisted of exchanging 250 mL of fresh perfusate at 1 h, and 100 mL, or the amount of perfusate loss if it was more than 100 mL/h, to the EVLP circuit every subsequent hour. Lower lobe bronchoalveolar lavage (BAL) with 30 mL of saline was performed at 1 h, before MSC[IL-10] administration, and at 12 h using a flexible fiberoptic bronchoscope and cOmplete, and supernatant and cell fractions were cryopreserved. Lower lobe lung wedge biopsies were taken with a stapler device (Covidien DST series GIA, Medtronic, Minneapolis, MN, USA) before EVLP start, and at 3, 6, and 9 h, and at the 12-h samples were taken from upper and lower lobe superficial (including parietal pleura) and deep areas (excluding parietal pleura). Lung tissue sample processing consisted of (1) snap freezing in liquid nitrogen, tissue homogenization, protein isolation,[13] and protein concentration measurement (Pierce bicinchoninic acid [BCA] protein assay kit, Thermo Fisher Scientific); (2) RNAlater RNA stabilization reagent (QIAGEN, Venlo, the Netherlands); (3) inflation and 24-h storage in 10% buffered formalin, change to 70% ethanol, and paraffin embedding; and (4) wet/dry lung weight ratio.

MSC[IL-10] administration during EVLP

For the treatment of human rejected lungs during EVLP, 40×10^6 MSC[IL-10] were thawed, reconstituted in 20 mL of EVLP perfusate solution (Steen solution, XVIVO Perfusion, Gothenburg, Sweden), and the cell viability was confirmed. MSC[IL-10] cells were administered with a syringe during 20 s through an extension tubing attached to the pulmonary artery cannula, followed by a 20-mL perfusate flush. Cell administration was performed after full perfusion flow, normothermia and lung ventilation had been achieved, and the 1-h lung assessment, and a baseline BAL sample followed by lung recruitment with two inspiratory holds with peak airway pressure 25 mmHg had been performed. Control group lungs were administered 20 mL of perfusate without cells.

Quantitative immunoassays

Perfusate, BAL, and lung IL-10 levels were determined with a human IL-10 Quantikine ELISA kit (R&D Systems, Minneapolis, MN, USA), and *in vitro* cell media IL-10 levels were determined with a human IL-10 DuoSet ELISA (R&D Systems). Perfusate cytokine panel analysis was performed with an Ella automated immunoassay system (R&D Systems) using 16×4 multianalyte cartridges for IL-1β, IL-6, IL-8, endothelin-1, GM-CSF, TNFR1, and TREM-1 (R&D Systems).

Immunostaining

Formalin-fixed, paraffin-embedded tissue sections (4 μm thick) were mounted on positively charged microscope slides. Antigen retrieval was performed with microwave heating in EDTA buffer (1 mmol/L EDTA, 0.05% Tween 20 [pH 9.0]). Endogenous peroxidase was blocked using 3% hydrogen peroxide. After blocking for 15 min with blocking buffer in a tyramine signal amplification kit (Alexa

Fluor 488 tyramide SuperBoost kit, Thermo Fisher Scientific, Waltham, MA, USA), rabbit anti-DDDDK tag (binds to FLAG tag sequence) primary antibody (ab205606, Abcam, Cambridge, UK) was applied overnight at 4°C, followed by the secondary antibody and the fluorescent detection step of the tyramine signal amplification kit. Slides were then washed and mounted with Vectashield mounting medium with 4′,6-diamidino-2-phenylindole (Vector Laboratories, Burlingame, CA, USA) and immediately imaged on a Quorum WaveFX spinning disk confocal microscope (Quorum Technologies, Puslinch, ON, Canada).

RNA extraction and quantitative RT-PCR to detect endogenous and transgenic IL-10 mRNA

Lung tissue samples collected in RNAlater were stored at −80°C. RNA was extracted using an RNA mini plus kit (QIAGEN) with extra DNase treatment and RNA clean-up to ensure there was no virus DNA contamination in the RNA samples. cDNA was synthesized from 1,000 ng of RNA using an iScript advanced cDNA synthesis kit (Bio-Rad, Hercules, CA, USA). qPCR was run on a CFX384 real-time system (Bio-Rad) using SsoAdvanced Universal SYBR Green supermix (Bio-Rad) and specific primers. Primers were designed according to the AdIL-10 construction information (Vigene Biosciences, no. VH869610). Gene expression was determined relative to Ppia housekeeping gene and the results were analyzed using the $\Delta\Delta$Ct method. Primers in the open reading frame, and in the 3′ untranslated region that is not present in AdIL-10, of IL-10 were used to detect endogenous IL-10 mRNA: forward primer, 5′-TGAAGAATGCCTTTAATAAGCTCCA-3′; reverse primer, 5′-GCCACCCTGATGTCTCAGTT-3′.

Primers in the open reading frame of IL-10, and in the FLAG area present only in the AdIL-10, were used to detect transgenic IL-10 mRNA: forward primer, 5′-ATGACAATGAAGATACGAAAC-3′; reverse primer, 5′-CGTCGTCATCCTTATAATC-3′.

Endotoxin assay and microbiological analysis

Endotoxin was determined from EVLP perfusate samples taken at 1 and 12 h using a Pierce chromogenic endotoxin quant kit (Thermo Fisher Scientific, Waltham, MA, USA). Microbiological quantitative culture and antibiotic sensitivity testing was performed from EVLP perfusate samples taken at 1 and 12 h in the hospital clinical laboratory (Department of Microbiology, Mount Sinai Hospital and the University Health Network, Toronto, ON, Canada).

MSC[IL-10] challenge with different metabolic conditions *in vitro*

The effect of metabolic factors on MSC[IL-10] IL-10 production was initially assessed by exposing MSC[IL-10] to nine different cryopreserved EVLP perfusate samples from control cases (collected from cases 1–3 at 1, 6, and 12 h) that had varying glucose, lactate, and pH levels (Figure 6A) and different cytokine profiles (Figure S5). MSC[IL-10] (3×10^6) were divided equally into nine tubes containing different perfusate sample. Tubes were fixed to a rotator placed in an incubator at 37°C, 5% CO_2 and samples were taken at 5 min, 30 min, and at 1, 2.5, and 4 h for IL-10 ELISA.

To further investigate the effects of glucose on IL-10 production, MSC^{IL-10} were cultured (n = 3) at 37°C, 5% CO_2 in DMEM media with high (25 mmol/L), low (5.5 mmol/L), or no glucose. Also, to assess the effects of pH, MSC^{IL-10} were cultured in standard perfusate solution (pH 7.40) or perfusate with pH 6.5, 5.9, 5.5, or 5.0 modified with hydrochloric acid. Samples were taken after 4 h to measure human IL-10 by ELISA and to determine cell viability using the Vi-CELL XR cell viability analyzer (Beckman Coulter, Brea, CA, USA).

Perfusate and tissue pH measurement

The point-of-care system (RAPIDPoint 500 blood gas system) used in each case to measure EVLP perfusate pH has a lower detection limit of pH 6.5. The pH value of perfusate samples collected from the damaged lungs used in the study dropped below the pH detection limit at some point during the EVLP in almost all cases. To achieve the full range of pH values for the *in vitro* experiments exposing MSC^{IL-10} to different perfusate samples and metabolic conditions (Figures 6A and 6E), stored samples were re-measured with a pH meter (Fisherbrand accumet AB150, Thermo Fisher Scientific) and pH microelectrode (Thermo Scientific Orion PerpHecT ROSS combination pH micro electrode, Thermo Fisher Scientific). In addition, the same pH meter and pH microelectrode were used to measure lung tissue interstitial pH from lung tissue samples that were freshly collected at the end of EVLP from four anatomical sites of the MSC^{IL-10}-treated lungs (upper lobe superficial, upper lobe deep, lower lobe superficial, and lower lobe deep areas), snap-frozen in liquid nitrogen, and stored in −80°C. The samples were thawed and stabilized to room temperature, and the pH meter was calibrated before each sample measurement.

pHrodo staining

pHrodo Red succinimidyl ester (P36600; Thermo Fisher Scientific) was used to visualize acidic areas in tissue sections. We performed preliminary experiments by incubating fresh tissue samples in pHrodo as described before.[33] As a similar pHrodo signal was also achieved by applying pHrodo directly on OCT-embedded (Thermo Fischer Scientific) tissue cryosections, we used this approach in the study. Snap-frozen lung tissue was embedded in OCT, and 10-μm cryosections were incubated for 5 min with pHrodo diluted 1:2,000 in distilled water, washed with distilled water, and then visualized with a Quorum WaveFX spinning disk confocal microscope (Quorum Technologies). Non-incubated lung cryosections served as negative controls, and a gastric tissue cryosection with pHrodo incubation was used as a positive control.

Statistical analysis

Data are expressed as median ± range or interquartile range and were analyzed with GraphPad Prism 8.4.1 (GraphPad, San Diego, CA, USA). Variables were compared by a Mann-Whitney test, or Kruskal-Wallis test, and the two-stage step-up method of Benjamini, Krieger, and Yekutieli was used for multiple comparisons. EVLP data with multiple time points were analyzed with two-way ANOVA with Sidak's multiple comparison test. Correlations were analyzed by linear regression and a Pearson coefficient test. $p < 0.05$ is considered statistically significant.

SUPPLEMENTAL INFORMATION

Supplemental information can be found online at https://doi.org/10.1016/j.omtm.2021.05.018.

AUTHOR CONTRIBUTIONS

A.I.N.: contributed to the concept and design of the experiments, performed EVLP experiments, sample and statistical analysis, and drafted and revised the manuscript; A.M.: contributed to the concept and design of the experiments and writing of the manuscript and performed EVLP experiments; A.D.: performed sample processing during EVLP experiments and performed FACS analysis; C.E.: manufactured, maintained, and characterized MSC^{IL-10} and performed *in vitro* experiments; A.A.: performed EVLP experiments; O.H.: performed EVLP experiments and LPS analysis; A.S. and B.T.C.: performed cytokine analysis; M.C., H.G., and H.S.: performed EVLP experiments; X.B.: performed sample processing and cytokine analysis; G.Z.: performed sample processing, pH measurements, and immunostainings; J.Y, T.W., T.M., S.J., M.C., and M.L.: participated in the study design, interpretation, and writing of the report; J.E.D.: principal investigator for manufacturing, maintenance, and characterization of MSC^{IL-10}, and *in vitro* experiments, and contributed to the concept and design of the experiments and writing of the report; S.K.: principal investigator of the study, designed the study, contributed in interpretation of the data and writing the report.

DECLARATION OF INTERESTS

C.E. is an employee of Tissue Regeneration Therapeutics Inc.; J.E.D is the CEO of Tissue Regeneration Therapeutics Inc.; S.J. and T.M. have received research support from Sanofi; T.W., M.C., M.L., and S.K. are owners of Perfusix Canada and XOR Labs Toronto. T.W., M.C., and S.K. are scientific medical advisors for Lung Bioengineering. The remaining authors declare no competing interests.

REFERENCES

1. Chambers, D.C., Cherikh, W.S., Harhay, M.O., Hayes, D., Jr., Hsich, E., Khush, K.K., Meiser, B., Potena, L., Rossano, J.W., Toll, A.E., et al.; International Society for Heart and Lung Transplantation (2019). The International Thoracic Organ Transplant Registry of the International Society for Heart and Lung Transplantation: Thirty-sixth adult lung and heart-lung transplantation report—2019; Focus theme: Donor and recipient size match. J. Heart Lung Transplant. *38*, 1042–1055.

2. Verleden, G.M., Glanville, A.R., Lease, E.D., Fisher, A.J., Calabrese, F., Corris, P.A., Ensor, C.R., Gottlieb, J., Hachem, R.R., Lama, V., et al. (2019). Chronic lung allograft dysfunction: Definition, diagnostic criteria, and approaches to treatment—A consensus report from the Pulmonary Council of the ISHLT. J. Heart Lung Transplant. *38*, 493–503.

3. Hachem, R.R. (2019). The role of the immune system in lung transplantation: Towards improved long-term results. J. Thorac. Dis. 11 (Suppl 14), S1721–S1731.

4. Rosenheck, J., Pietras, C., and Cantu, E. (2018). Early graft dysfunction after lung transplantation. Curr. Pulmonol. Rep. 7, 176–187.

5. Chan, P.G., Kumar, A., Subramaniam, K., and Sanchez, P.G. (2020). Ex vivo lung perfusion: A review of research and clinical practices. Semin. Cardiothorac. Vasc. Anesth. 24, 34–44.

6. Cypel, M., Yeung, J.C., Liu, M., Anraku, M., Chen, F., Karolak, W., Sato, M., Laratta, J., Azad, S., Madonik, M., et al. (2011). Normothermic ex vivo lung perfusion in clinical lung transplantation. N. Engl. J. Med. 364, 1431–1440.

7. Divithotawela, C., Cypel, M., Martinu, T., Singer, L.G., Binnie, M., Chow, C.W., Chaparro, C., Waddell, T.K., de Perrot, M., Pierre, A., et al. (2019). Long-term outcomes of lung transplant with ex vivo lung perfusion. JAMA Surg. 154, 1143–1150.

8. Machuca, T.N., Hsin, M.K., Ott, H.C., Chen, M., Hwang, D.M., Cypel, M., Waddell, T.K., and Keshavjee, S. (2013). Injury-specific ex vivo treatment of the donor lung: Pulmonary thrombolysis followed by successful lung transplantation. Am. J. Respir. Crit. Care Med. 188, 878–880.

9. Tane, S., Noda, K., and Shigemura, N. (2017). Ex vivo lung perfusion: A key tool for translational science in the lungs. Chest 151, 1220–1228.

10. Rahim, F., and Ebrahimi, A. (2014). Gene therapy modalities in lung transplantation. Transpl. Immunol. 31, 165–172.

11. Shirley, J.L., de Jong, Y.P., Terhorst, C., and Herzog, R.W. (2020). Immune responses to viral gene therapy vectors. Mol. Ther. 28, 709–722.

12. de Perrot, M., Fischer, S., Liu, M., Imai, Y., Martins, S., Sakiyama, S., Tabata, T., Bai, X.H., Waddell, T.K., Davidson, B.L., and Keshavjee, S. (2003). Impact of human interleukin-10 on vector-induced inflammation and early graft function in rat lung transplantation. Am. J. Respir. Cell Mol. Biol. 28, 616–625.

13. Yeung, J.C., Wagnetz, D., Cypel, M., Rubacha, M., Koike, T., Chun, Y.-M., Hu, J., Waddell, T.K., Hwang, D.M., Liu, M., and Keshavjee, S. (2012). Ex vivo adenoviral vector gene delivery results in decreased vector-associated inflammation pre- and post-lung transplantation in the pig. Mol. Ther. 20, 1204–1211.

14. Cypel, M., Liu, M., Rubacha, M., Yeung, J.C., Hirayama, S., Anraku, M., Sato, M., Medin, J., Davidson, B.L., de Perrot, M., et al. (2009). Functional repair of human donor lungs by IL-10 gene therapy. Sci. Transl. Med. 1, 4ra9.

15. Almeida-Porada, G., Atala, A.J., and Porada, C.D. (2020). Therapeutic mesenchymal stromal cells for immunotherapy and for gene and drug delivery. Mol. Ther. Methods Clin. Dev. 16, 204–224.

16. Bari, E., Ferrarotti, I., Torre, M.L., Corsico, A.G., and Perteghella, S. (2019). Mesenchymal stem/stromal cell secretome for lung regeneration: The long way through "pharmaceuticalization" for the best formulation. J. Control. Release 309, 11–24.

17. Vandermeulen, M., Erpicum, P., Weekers, L., Briquet, A., Lechanteur, C., Detry, O., Beguin, Y., and Jouret, F. (2020). Mesenchymal stromal cells in solid organ transplantation. Transplantation 104, 923–936.

18. Chambers, D.C., Enever, D., Lawrence, S., Sturm, M.J., Herrmann, R., Yerkovich, S., Musk, M., and Hopkins, P.M. (2017). Mesenchymal stromal cell therapy for chronic lung allograft dysfunction: Results of a first-in-man study. Stem Cells Transl. Med. 6, 1152–1157.

19. Keller, C.A., Gonwa, T.A., Hodge, D.O., Hei, D.J., Centanni, J.M., and Zubair, A.C. (2018). Feasibility, safety, and tolerance of mesenchymal stem cell therapy for obstructive chronic lung allograft dysfunction. Stem Cells Transl. Med. 7, 161–167.

20. Gupta, N., Su, X., Popov, B., Lee, J.W., Serikov, V., and Matthay, M.A. (2007). Intrapulmonary delivery of bone marrow-derived mesenchymal stem cells improves survival and attenuates endotoxin-induced acute lung injury in mice. J. Immunol. 179, 1855–1863.

21. Lee, J.W., Fang, X., Gupta, N., Serikov, V., and Matthay, M.A. (2009). Allogeneic human mesenchymal stem cells for treatment of E. coli endotoxin-induced acute lung injury in the ex vivo perfused human lung. Proc. Natl. Acad. Sci. USA 106, 16357–16362.

22. Lee, J.W., Krasnodembskaya, A., McKenna, D.H., Song, Y., Abbott, J., and Matthay, M.A. (2013). Therapeutic effects of human mesenchymal stem cells in ex vivo human lungs injured with live bacteria. Am. J. Respir. Crit. Care Med. 187, 751–760.

23. Islam, D., Huang, Y., Fanelli, V., Delsedime, L., Wu, S., Khang, J., Han, B., Grassi, A., Li, M., Xu, Y., et al. (2019). Identification and modulation of microenvironment is crucial for effective mesenchymal stromal cell therapy in acute lung injury. Am. J. Respir. Crit. Care Med. 199, 1214–1224.

24. Zheng, G., Huang, L., Tong, H., Shu, Q., Hu, Y., Ge, M., Deng, K., Zhang, L., Zou, B., Cheng, B., and Xu, J. (2014). Treatment of acute respiratory distress syndrome with allogeneic adipose-derived mesenchymal stem cells: A randomized, placebo-controlled pilot study. Respir. Res. 15, 39.

25. Wilson, J.G., Liu, K.D., Zhuo, H., Caballero, L., McMillan, M., Fang, X., Cosgrove, K., Vojnik, R., Calfee, C.S., Lee, J.W., et al. (2015). Mesenchymal stem (stromal) cells for treatment of ARDS: A phase 1 clinical trial. Lancet Respir. Med. 3, 24–32.

26. Matthay, M.A., Calfee, C.S., Zhuo, H., Thompson, B.T., Wilson, J.G., Levitt, J.E., Rogers, A.J., Gotts, J.E., Wiener-Kronish, J.P., Bajwa, E.K., et al. (2019). Treatment with allogeneic mesenchymal stromal cells for moderate to severe acute respiratory distress syndrome (START study): A randomised phase 2a safety trial. Lancet Respir. Med. 7, 154–162.

27. Simonson, O.E., Mougiakakos, D., Heldring, N., Bassi, G., Johansson, H.J., Dalén, M., Jitschin, R., Rodin, S., Corbascio, M., El Andaloussi, S., et al. (2015). In vivo effects of mesenchymal stromal cells in two patients with severe acute respiratory distress syndrome. Stem Cells Transl. Med. 4, 1199–1213.

28. Leng, Z., Zhu, R., Hou, W., Feng, Y., Yang, Y., Han, Q., Shan, G., Meng, F., Du, D., Wang, S., et al. (2020). Transplantation of ACE2− mesenchymal stem cells improves the outcome of patients with COVID-19 pneumonia. Aging Dis. 11, 216–228.

29. Zhou, P., Yang, X.L., Wang, X.G., Hu, B., Zhang, L., Zhang, W., Si, H.R., Zhu, Y., Li, B., Huang, C.L., et al. (2020). A pneumonia outbreak associated with a new coronavirus of probable bat origin. Nature 579, 270–273.

30. Mordant, P., Nakajima, D., Kalaf, R., Iskender, I., Maahs, L., Behrens, P., Coutinho, R., Iyer, R.K., Davies, J.E., Cypel, M., et al. (2016). Mesenchymal stem cell treatment is associated with decreased perfusate concentration of interleukin-8 during ex vivo perfusion of donor lungs after 18-hour preservation. J. Heart Lung Transplant. 35, 1245–1254.

31. Nakajima, D., Watanabe, Y., Ohsumi, A., Pipkin, M., Chen, M., Mordant, P., Kanou, T., Saito, T., Lam, R., Coutinho, R., et al. (2019). Mesenchymal stromal cell therapy during ex vivo lung perfusion ameliorates ischemia-reperfusion injury in lung transplantation. J. Heart Lung Transplant. 38, 1214–1223.

32. Dominici, M., Le Blanc, K., Mueller, I., Slaper-Cortenbach, I., Marini, F., Krause, D., Deans, R., Keating, A., Prockop, Dj., and Horwitz, E. (2006). Minimal criteria for defining multipotent mesenchymal stromal cells. The International Society for Cellular Therapy position statement. Cytotherapy 8, 315–317.

33. Liu, C.L., Zhang, X., Liu, J., Wang, Y., Sukhova, G.K., Wojtkiewicz, G.R., Liu, T., Tang, R., Achilefu, S., Nahrendorf, M., et al. (2019). Na+-H+ exchanger 1 determines atherosclerotic lesion acidification and promotes atherogenesis. Nat. Commun. 10, 3978.

34. Han, J., and Burgess, K. (2010). Fluorescent indicators for intracellular pH. Chem. Rev. 110, 2709–2728.

35. Shahryari, A., Saghaeian Jazi, M., Mohammadi, S., Razavi Nikoo, H., Nazari, Z., Hosseini, E.S., Burtscher, I., Mowla, S.J., and Lickert, H. (2019). Development and clinical translation of approved gene therapy products for genetic disorders. Front. Genet. 10, 868.

36. Panés, J., García-Olmo, D., Van Assche, G., Colombel, J.F., Reinisch, W., Baumgart, D.C., Dignass, A., Nachury, M., Ferrante, M., Kazemi-Shirazi, L., et al.; ADMIRE CD Study Group Collaborators (2016). Expanded allogeneic adipose-derived mesenchymal stem cells (Cx601) for complex perianal fistulas in Crohn's disease: A phase 3 randomised, double-blind controlled trial. Lancet 388, 1281–1290.

37. Han, J., Liu, Y., Liu, H., and Li, Y. (2019). Genetically modified mesenchymal stem cell therapy for acute respiratory distress syndrome. Stem Cell Res. Ther. 10, 386.

38. Manning, E., Pham, S., Li, S., Vazquez-Padron, R.I., Mathew, J., Ruiz, P., and Salgar, S.K. (2010). Interleukin-10 delivery via mesenchymal stem cells: A novel gene therapy approach to prevent lung ischemia-reperfusion injury. Hum. Gene Ther. 21, 713–727.

39. Podestà, M.A., Remuzzi, G., and Casiraghi, F. (2019). Mesenchymal stromal cells for transplant tolerance. Front. Immunol. 10, 1287.

40. Machuca, T.N., Cypel, M., Bonato, R., Yeung, J.C., Chun, Y.M., Juvet, S., Guan, Z., Hwang, D.M., Chen, M., Saito, T., et al. (2017). Safety and efficacy of ex vivo donor

lung adenoviral IL-10 gene therapy in a large animal lung transplant survival model. Hum. Gene Ther. *28*, 757–765.

41. Fischer, S., Liu, M., MacLean, A.A., de Perrot, M., Ho, M., Cardella, J.A., Zhang, X.M., Bai, X.H., Suga, M., Imai, Y., and Keshavjee, S. (2001). In vivo transtracheal adenovirus-mediated transfer of human interleukin-10 gene to donor lungs ameliorates ischemia-reperfusion injury and improves early posttransplant graft function in the rat. Hum. Gene Ther. *12*, 1513–1526.

42. Wang, C., Lv, D., Zhang, X., Ni, Z.A., Sun, X., and Zhu, C. (2018). Interleukin-10-overexpressing mesenchymal stromal cells induce a series of regulatory effects in the inflammatory system and promote the survival of endotoxin-induced acute lung injury in mice model. DNA Cell Biol. *37*, 53–61.

43. Martínez-González, I., Roca, O., Masclans, J.R., Moreno, R., Salcedo, M.T., Baekelandt, V., Cruz, M.J., Rello, J., and Aran, J.M. (2013). Human mesenchymal stem cells overexpressing the IL-33 antagonist soluble IL-1 receptor-like-1 attenuate endotoxin-induced acute lung injury. Am. J. Respir. Cell Mol. Biol. *49*, 552–562.

44. He, H., Liu, L., Chen, Q., Liu, A., Cai, S., Yang, Y., Lu, X., and Qiu, H. (2015). Mesenchymal stem cells overexpressing angiotensin-converting enzyme 2 rescue lipopolysaccharide-induced lung injury. Cell Transplant. *24*, 1699–1715.

45. Naidu, B.V., Krishnadasan, B., Farivar, A.S., Woolley, S.M., Thomas, R., Van Rooijen, N., Verrier, E.D., and Mulligan, M.S. (2003). Early activation of the alveolar macrophage is critical to the development of lung ischemia-reperfusion injury. J. Thorac. Cardiovasc. Surg. *126*, 200–207.

46. Fernandez, S., Jose, P., Avdiushko, M.G., Kaplan, A.M., and Cohen, D.A. (2004). Inhibition of IL-10 receptor function in alveolar macrophages by Toll-like receptor agonists. J. Immunol. *172*, 2613–2620.

47. Athanasopoulos, T., Munye, M.M., and Yáñez-Muñoz, R.J. (2017). Nonintegrating gene therapy vectors. Hematol. Oncol. Clin. North Am. *31*, 753–770.

48. Gramlich, O.W., Burand, A.J., Brown, A.J., Deutsch, R.J., Kuehn, M.H., and Ankrum, J.A. (2016). Cryopreserved mesenchymal stromal cells maintain potency in a retinal ischemia/reperfusion injury model: Toward an off-the-shelf therapy. Sci. Rep. *6*, 26463.

49. Noronha, N.C., Mizukami, A., Caliári-Oliveira, C., Cominal, J.G., Rocha, J.L.M., Covas, D.T., Swiech, K., and Malmegrim, K.C.R. (2019). Priming approaches to improve the efficacy of mesenchymal stromal cell-based therapies. Stem Cell Res. Ther. *10*, 131.

50. Kan, C., Chen, L., Hu, Y., Lu, H., Li, Y., Kessler, J.A., and Kan, L. (2017). Microenvironmental factors that regulate mesenchymal stem cells: Lessons learned from the study of heterotopic ossification. Histol. Histopathol. *32*, 977–985.

51. Drachman, N., Kadlecek, S., Pourfathi, M., Xin, Y., Profka, H., and Rizi, R. (2017). In vivo pH mapping of injured lungs using hyperpolarized [1-^{13}C]pyruvate. Magn. Reson. Med. *78*, 1121–1130.

52. Moon, C.M., Kim, Y.H., Ahn, Y.K., Jeong, M.H., and Jeong, G.W. (2019). Metabolic alterations in acute myocardial ischemia-reperfusion injury and necrosis using in vivo hyperpolarized [1-^{13}C] pyruvate MR spectroscopy. Sci. Rep. *9*, 18427.

53. Potts, D.E., Taryle, D.A., and Sahn, S.A. (1978). The glucose-pH relationship in parapneumonic effusions. Arch. Intern. Med. *138*, 1378–1380.

54. Torres, I.M., Patankar, Y.R., and Berwin, B. (2018). Acidosis exacerbates in vivo IL-1-dependent inflammatory responses and neutrophil recruitment during pulmonary *Pseudomonas aeruginosa* infection. Am. J. Physiol. Lung Cell. Mol. Physiol. *314*, L225–L235.

55. Shah, V.S., Meyerholz, D.K., Tang, X.X., Reznikov, L., Abou Alaiwa, M., Ernst, S.E., Karp, P.H., Wohlford-Lenane, C.L., Heilmann, K.P., Leidinger, M.R., et al. (2016). Airway acidification initiates host defense abnormalities in cystic fibrosis mice. Science *351*, 503–507.

56. Gessner, C., Hammerschmidt, S., Kuhn, H., Seyfarth, H.J., Sack, U., Engelmann, L., Schauer, J., and Wirtz, H. (2003). Exhaled breath condensate acidification in acute lung injury. Respir. Med. *97*, 1188–1194.

57. Anemone, A., Consolino, L., Arena, F., Capozza, M., and Longo, D.L. (2019). Imaging tumor acidosis: A survey of the available techniques for mapping in vivo tumor pH. Cancer Metastasis Rev. *38*, 25–49.

58. Eppinger, M.J., Ward, P.A., Bolling, S.F., and Deeb, G.M. (1996). Regulatory effects of interleukin-10 on lung ischemia-reperfusion injury. J. Thorac. Cardiovasc. Surg. *112*, 1301–1305, discussion 1305–1306.

59. Zhao, M., Fernandez, L.G., Doctor, A., Sharma, A.K., Zarbock, A., Tribble, C.G., Kron, I.L., and Laubach, V.E. (2006). Alveolar macrophage activation is a key initiation signal for acute lung ischemia-reperfusion injury. Am. J. Physiol. Lung Cell. Mol. Physiol. *291*, L1018–L1026.

60. Cypel, M., and Keshavjee, S. (2014). Ex vivo lung perfusion. Oper. Tech. Thorac. Cardiovasc. Surg. *19*, 433–442.